This is a repository copy of *Influence of Fuel Injection Location in a Small Radial Swirler Low NO$_x$ Combustor for Micro Gas Turbine Applications*.

White Rose Research Online URL for this paper:
http://eprints.whiterose.ac.uk/160337/

Version: Accepted Version

GT2019-90197

INFLUENCE OF FUEL INJECTION LOCATION IN A SMALL RADIAL SWIRLER LOW NO$_X$ COMBUSTOR FOR MICRO GAS TURBINE APPLICATIONS

Gordon E. Andrews and Myeong Kim

School of Chemical and Process Engineering
University of Leeds, Leeds, LS2 9JT, UK

ABSTRACT

The influence of fuel injection location in a low NO$_x$ (1) micro-gas turbine [MGT] in the ~50kWe (kW electric) size range was investigated, for NG and propane, to extend the power turn down using a pilot fuel injector. The low NO$_x$ main combustor (1) was a radial swirler with vane passage fuel injection and had ultra-low NOx emissions of 3ppm at 15% O$_2$ at 1800K with natural gas, NG at a combustion intensity of 11.2 MW/m^{2}bara (MW thermal). This was a 40mm diameter outlet eight bladed radial swirler in a 76mm diameter combustor, investigated at 740K air temperature at atmospheric pressure. However, power turn down was poor and the present work was undertaken to determine the optimum position of pilot fuel injection that would enable leaner mixtures to be burned at low powers. Central injection of pilot fuel was investigated using 8 radial outward holes. This was compared with pilot fuel injected at the 76mm wall just downstream of the 40mm swirler outlet. It was show that the central injection pilot was poor with a worse weak extinction than for radial passage fuel injection. The 76mm outlet wall injection was much more successful as a pilot fuel location and had a weak extinction of 0.18Ø compared with 0.34Ø for vane passage fuel injection. NO$_x$ emissions were higher for wall fuel injection, but were still relatively low at 16ppm at 15% oxygen for natural gas. This indicates that wall fuel injection could be combined with vane passage fuel injection to improve the micro-gas turbine low NO$_x$ performance across the power range.

INTRODUCTION

There is a growing interest in micro-gas turbines [MGT] for distributed electric power production. The local generation of electricity, close to its intended use, avoids the typically 8% thermal efficiency**,** η$_{th}$**,** loss of conventional high voltage power distribution from large GW+ power generator sites to the customer (2). Also, they can be used alongside renewable energy, such as solar, to give continuous local power generation (3, 4). They have multi-fuel capability and with biomass (5, 6) and in a biogas/solar/mgt system (7) offers completely renewable electricity throughout the day. For low cost MGTs automotive turbochargers are being used with a cylindrical combustor connecting the compressor and turbine (8). For improved cycle thermal efficiency recuperated MGT are used (9). In the present work recuperator MGT combustors are simulated using an inlet air temperature of 740K.

MGT combustors can be annular (10) or a single cylindrical combustor (8, 11). The cylindrical combustors have advantages in terms of the lower surface to volume ratio for wall cooling and they are easier to remove for maintenance. The cylindrical combustor is the only one suitable for matching to automotive turbochargers. Vick et al. (9) have also shown that a cylindrical combustor can be used in a compact recuperated MGT with a central blockage of the combustor outlet to generate an annular feed into the turbine.

Andrews and Kim (1) have previously shown that the present 40mm outlet radial swirler with radial vane fuel injection [8 vanes and 8 fuel injectors, one at the inlet to each vane passage] (12-16) had ultra-low NO$_x$ emissions of 3ppm at 15% oxygen with natural gas [NG]. This type of low NO$_x$ GT combustor is used in eight production gas turbines in the 0.25–60 MWe [MW electric] range (27-31). This is similar to some existing MGT designs (10, 17-20), but all these designs have swirlers that are too small relative to their enclosure if the swirlers were to pass a large proportion of the total combustion air (12). Small combustors for gas turbines, of the size used in the present work, may also be used as pilot well mixed burners in the centre of a larger radial or axial swirler array (16, 21).

Andrews and Kim (1) investigated a 40mm outlet eight bladed radial swirler for four radial swirler vane depths from 30.5mm to 12.2mm and a constant pressure loss of 2.7% at

different reference Mach numbers or residence times. For a 740K inlet temperature and 0.6 equivalence ratio, Ø, these gave combustor thermal loadings at atmospheric pressure from 33 to 62 kW and heat release of 7 – 14 MW/m²bara. The MW here are MW thermal and the ratio of MWe to MW thermal is the thermal efficiency, η_{th}.

The vane passage single hole fuel injection achieved NOx emissions of 1–5ppm at 15% oxygen, 740K air inlet temperature and 1700K primary zone temperature, with <10ppm CO. The 1ppm NOx was for the smallest vane depth and lowest thermal power. The higher NO_x for the larger heat release swirler designs were due to the longer flame development and a greater formation of prompt NO_x, due to the high total hydrocarbon [THC] emissions for most of the flame development.

Andrews and Kim (1) found that the flame weak extinction with radial vane passage fuel injection was close to that of a premixed system and the power turndown was low if 1-3ppm NO_x was to be achieved at full power. The present work was undertaken to extend the weak extinction and power turndown using different fuel injection locations. An eight hole radially outward central fuel injector and an eight hole radially inward fuel injector at the 76mm combustor wall, just downstream of the radial swirler outlet plane, were compared with the original vane passage fuel injection. It will be shown that only the outer wall fuel injector demonstrated a significant improvement in the weak extinction and this was the preferred design for a pilot/main fueling system.

RADIAL SWIRLER DESIGN

The original radial swirler design of AlKabie and Andrews (13-15) was for a 140mm combustor with a 76mm radial swirler outlet diameter. The thermal power and combustion intensity was varied by changing the combustor flow rate at the same pressure loss by increasing the vane depth, with no change in the outlet diameter, d, or the combustor diameter, D (22-24). The combustor reference Mach number, M_1, was increased as the vane depth was increased for the same pressure loss. The reference Mach number, M_1, is based on the mean velocity in the combustor at the air inlet temperature.

For a 740K air inlet temperature, a CV of 50 MJ/kg for methane and a low NO_x condition with Ø=0.6 the combustion intensity is 11.2 MW/m²bara for a primary zone Mach number of 0.027, corresponding to 54% of the combustion air passing through the swirler. Andrews and Kim (1) compared four 40mm outlet diameter radial swirlers in a 76mm diameter combustor, which was 30% of the combustor flow area of the original 140mm diameter combustor with a similar combustor to swirler outlet diameter ratio, D/d, or expansion ratio of 1.9. For the same radial swirler vane angle this would give the same inner and outer recirculation zones so that the aerodynamics were scaled. They showed that for vane passage fuel injection very low NO_x could be achieved in the 40mm outlet diameter radial swirlers, which were similar to the NO_x from the original
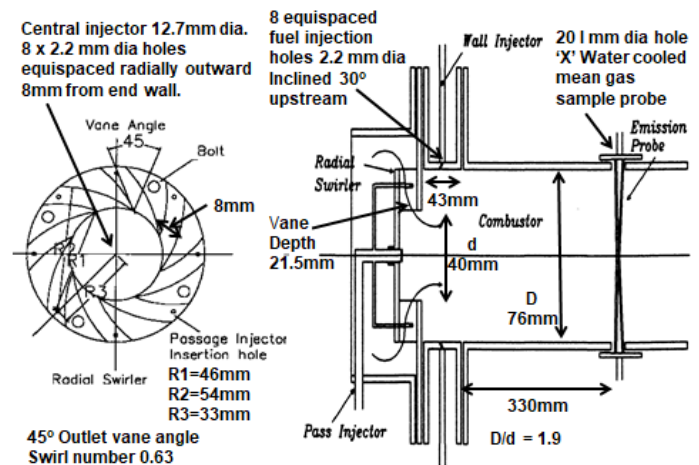

Figure 1 Radial swirler geometrical configuration.

larger radial swirlers (13-15, 22, 23). This smaller radial swirler size gives the basis for ultra-low NO_x MGT applications.

In the present work the small radial swirler A2, which was one of the four radial swirlers investigated by Andrews and Kim (1), was used to investigate the influence of the fuel injection location on NO_x and weak extinction. The detailed design of the radial swirler A2 is shown in Fig. 1. It is a 45° 8 vane passage radial swirler with an outlet diameter, d, of 40mm and a combustor diameter, D, of 76mm. The vane passage flow area A_2 is 8Lh and can be varied by changing the vane depth, L, which was 21.5mm for radial swirler A2. At the design pressure loss of 2.7% and reference Mach number of 0.027 the combustion intensity was 11.2 MW/(bar m²) which has a thermal power for methane at one bara of 51.7 kW for Ø=0.6. A single combustor for MGT applications with a pressure of 5 bara (25, 26) and simple cycle thermal efficiency, η_{th} of 0.3 (5, 26), would give a MGT with 77kWe (kW electric) power output.

The primary zone length was 330mm which was the same as in the work of Alkabie and Andrews (13-15) for the larger 140mm diameter combustor. No dilution air was used and only the low NO_x primary zone combustion was investigated. The primary zone was operated at an equivalence ratio that would achieve low NO_x and low CO with around 1800K at full engine power. The proportion of air in the primary zone that was simulated is the ratio of the primary reference Mach number, 0.027, to the overall reference Mach number for all the air flow of typically 0.05. This is 54% primary air and 46% dilution plus any downstream cooling air. Essentially this models turbine entry temperatures <1800K. For 740K inlet temperature the primary zone ΔT was 1060K and 46% dilution would give 1312K turbine entry temperature for swirler A2. Current production MGTs operate at 1173K and 1223K TIT (3). Experimental designs use TITs of 1011K (26), 1100K (25), 1218K (9), 1250K (18), 1397K (17) and 1500K (10). The

present simulated TIT of 1312K is thus representative of modern MGTs.

The 76mm combustor diameter is smaller than is used in some MGTs, such as the 90mm of Vick et al. (9) for an 11kWe MGT at 21% net thermal efficiency and a pressure ratio of 2.35. This is a combustion intensity of 1.33 MW/m^2bara, which is much lower than in the present work where the combustion intensity is 11.2 MW/m^2bara. This shows that the combustor is significantly bigger and heavier than it needs to be. This is also a feature of the MGT investigated by Monz et al. (18), where the heat release was 3.5 MW/m^2bara at 92% of full power. All these heat release rates are well below those studied in the present work, due to the use of over large combustors. Overlarge combustors also penalise the NO_x emissions as the larger residence times can give rise to increased thermal NO_x.

A feature of the design in Fig. 1, that was also used in the original work of Alkabie and Andrews (13-15), was the dump flow expansion from the exit of the swirler, with only the thickness of the combustor front face as a discharge duct. This design has the advantage of the flow through the radial passages cooling the combustor head. Most applications of radial swirlers in industry have not used this design feature and have added a discharge duct to aid fuel and air mixing, as in the work of Armstrong et al. (11), Fischer et al. (27) and Boyns and Patel (28). This type of design then usually uses effusion cooling of the back face of the combustor, which compromises the NO_x emissions, as less air is available for lean combustion.

Alkabie and Andrews (15) showed that the most effective use of a discharge duct from the radial swirler outlet was to mount fuel injectors on the wall, so that no fuel was added in the vane passage and thus flashback could not possibly occur. Very low NO_x emissions were demonstrated (15, 23) for gas and liquid fuels with this location for the fuel injection. In the present work this location for fuel injection would be a 40mm diameter outlet duct, which would have no advantage for NO_x and would add to the length and weight of the combustor. Also MGT operating conditions are rarely such that flashback into the radial vane passages would occur.

Instead of injecting fuel at the radial swirler outlet wall, this work used a radial wall fuel injector at the 76mm combustor wall to act as a pilot fuel staged zone in the outer corner recirculation zone created in dump expansion swirl flow. This fuel injector location has been shown by Alkabie and Andrews (29) to act as a pilot and to enhance the flame stability and power turndown of the 76mm outlet radial swirlers. The penalty was an increase in NO_x, but at low powers this could be acceptable.

Alkabie and Andrews (29) also showed that a central fuel injector with 8 radial fuel holes could also act as a pilot and this was investigated for the present scaled down MGT combustor. The location of all three fuel injection locations is shown in Fig. 1. For all locations 8 fuel holes of 2.2mm diameter were used. For the radial vane passages only one fuel hole per vane passage was used, as this gave good mixing with low NO_x in the 140mm combustor and more complex fueling systems were

not justified, but have generally been used in industrial applications of radial swirlers (11, 27, 28, 30).

Another key feature of low NO_x radial swirlers, that is used by most of the manufacturers (27-31), is for the centre of the swirler to be open, which enables the central recirculation zone to go back inside the swirler and impinge on the rear wall of the radial swirler. This is fundamental to the good flame stability and low acoustic resonance problems encountered in this design. The hot recirculated burned gases are entrained into the outlet flow from the radial swirler passages and this acts to stabilize the flame. Where this central reverse flow has been stopped by the insertion of a separate pilot zone by some manufacturers, flame instability and acoustic resonance problems have been encountered (30, 31, and 32).

EXPERIMENTAL EQUIPMENT

The experimental radial swirler test configuration is shown schematically in Fig. 1. Electrical air preheat was used to achieve the combustor air temperatures of 740K, which simulates micro gas turbine regenerative heating combustor inlet temperatures. Air was supplied at atmospheric pressure from a centrifugal fan and metered using a venturi differential pressure ISO standard flow meter accurate to 1% of the reading. The air mass flow was set to achieve a reference Mach number, M_1, of 0.027 and a pressure loss of 2.7%. The measured radial swirler flow discharge coefficient, C_d, was 0.40. The combustion intensity was 11.2 MW/m^2bara. The fuel flow was measured using a variable area flow meter with 2% flow resolution.

Atmospheric combustion testing for gas turbine has a long history and it is now accepted by most manufacturers that new low NO_x combustors should be developed first at atmospheric pressure and any NO_x problem solved at this low cost stage, before committing to full high pressure or engine tests. The tests at atmospheric pressure of the primary zone of low NO_x combustors has been validated by industrial users of the radial swirler design of low NO_x combustors where all have found low NO_x emissions (11, 27, 28, 30) as was originally found by Alkabie and Andrews (12-15). The investigating of the primary zone only has also been validated in the above work. Provided the primary zone combustion is complete, as shown in the present work with combustion inefficiencies <0.1%, then the addition of dilution air does not change CO or UHC or NO_x when corrected to a reference oxygen level.

A 20 hole water cooled mean gas sample probe was located at the combustor exit plane, 330mm downstream of the radial swirler outlet. With the 76mm diameter wall fuel injector in place this distance increases to 373mm. This mean gas sample was transported through heated sample lines to an emissions measurement system for NO_x, CO, THC and oxygen analysis. The analytical techniques used in the analysers was chemiluminescence for NO_x, non-dispersive infra-red (NDIR) for CO and CO_2, flame ionization detection (FID) for total hydrocarbons (THC) and paramagnetic analysis for oxygen.

The combustion equivalence ratio, Ø, was calculated based on a carbon balance from the CO_2, CO and THC measurements. All the experimental results are plotted as a function of Ø by carbon balance. The equivalence ratio, Ø, by carbon balance agreed to within 10% with the metered Ø. A better agreement could have been achieved if more sample holes were used, but practically 20 in a water cooled 'X' probe for the 76mm diameter combustor was the limit of our manufacturing capabilities. The gas sample was transported to the analysers using heated sample lines and for the NDIR and paramagnetic analysers the sample was cooled and the water extracted so that a dry gas analysis was obtained. The NO_x and THC were measured hot with the water vapour present, so that no loss of sample occurred. The combustion inefficiency was computed from the energy content of the measured CO and THC.

WEAK EXTINCTION RESULTS

The test rig exhaust system had an air cooled window in the exhaust on the centreline of the swirler, which was about 2m upstream of the window. The weak extinction was determined by observing the flame as the fuel flow was reduced at constant air flow. The sudden weak extinction was accompanied by a large increase in THC and CO emissions. The weak extinction equivalence ratios are given in Table 1, together with the adiabatic flame temperature at weak extinction, which is referred to as the critical temperature for flame stability.

Table 1 Radial Swirler A2 Weak Extinction, $Ø_{WE}$, at a Pressure Loss of 2.7% at $M_1 = 0.027$, U_1 13.6 m/s and 11.2 MW/m^2bar

Fuel injection	Fuel	Air T K	$Ø_{WE}$	WE Flame Temp. K
Passage (1)	NG	740	0.34	1513
Passage (1)	NG	600	0.45	1607
Passage (1)	P	740	0.33	1509
Passage (1)	P	600	0.43	1591
Wall	NG	740	0.18	1128
Wall	NG	600	0.22	1180
Wall	P	740	0.18	1084
Wall	P	600	0.21	1119
Central	NG	740	0.40	1600
LEL	P	740	0.30	1400
LEL	P	600	0.32	1400

Andrews et al. (33) reviewed published weak extinction data for experimental low NO_x combustors. 128 experimental weak extinction data points from low NO_x GT research and some engine data were reviewed. 21 weak extinction measurements (16% of all the data) were in the critical temperature range of 1400 – 1500K, close to the lean flammability limit (33) shown in Table 1. 53% of the published data had a critical temperature in the range 1500 – 1600K.

Table 1 shows that the present radial vane passage fuel injection weak extinction measurements are all in the critical temperature range 1500K – 1600K range. Also the one central fuel injection weak extinction had a 1600K critical temperature. This shows that these downsized radial swirlers operated in a near premixed mode with flame stability close to the fundamental lean flammability limits.

The central fuel injection result was surprising, as in the 140mm radial swirler combustion tests this location had acted as a pilot with much leaner weak extinction than in Table 1(29). Central fuel injection had a worse weak extinction than for vane passage fuel injection and one that was significantly richer than the lower explosion limit (LEL). The reason was due to the deeper radial vanes used, compared with those used in the 140mm combustor. This placed the central fuel injection further from the swirler flow expansion turbulent shear layer, which stabilized the flame, and thus gave more time for fuel and air mixing to occur. The weak extinction results show that the central fuel injector and location was not useful as a pilot, as the weak extinction was richer than for vane passage fuel injection.

Table 1 shows that the 76mm wall injection location, shown in Fig. 1, had weak extinction results much leaner than that for vane passage or central fuel injection. The critical flame temperature was about 1150K for NG at 600-740K. This shows that the 76mm wall injector could be a good location for the injection of pilot fuel or for staged fuel injection at low powers.

COMBUSTION INEFFICIENCY RESULTS

The combustion inefficiency is the sum of the energy content of the unburned CO and total hydrocarbons (THC) as a ratio of the energy input from the fuel flow. An inefficiency <0.1% would be required for a thermally efficient micro gas turbines. In order to calculate the combustion inefficiency, the CO and THC volumetric concentrations in Figs. 2 and 3 were converted to an Emission Index [EI] in g/kg_{fuel}. The EI_{CO} is then multiplied by the ratio of the GCV for CO and the fuel GCV to give the combustion inefficiency for CO. The THC combustion inefficiency is the EI_{THC} multiplied by the ratio of the GCV for THC (taken as methane) and the fuel GCV, which is unity for NG. The CO and THC combustion inefficiencies are then added to give the overall combustion inefficiency. The combustion inefficiency results are shown in Fig. 4 as a function of Ø.

Fig. 2 shows the CO volumetric emissions as a function of Ø for 740K inlet air temperature. This shows that for all methods of fueling and for both fuels the CO emissions were close to equilibrium for Ø > 0.5. Fig. 2 shows that there was a critical equivalence ratio for the minimum CO and for leaner mixtures the CO increased markedly, as there was insufficient time in the fixed length primary zone for the combustion to reach equilibrium. The Ø region between the minimum CO and the weak extinction was a region of stable combustion with high CO emissions. Fig. 3 shows similar results for THC, with ~1ppm for Ø > 0.5, with a sharp increase in THC for leaner
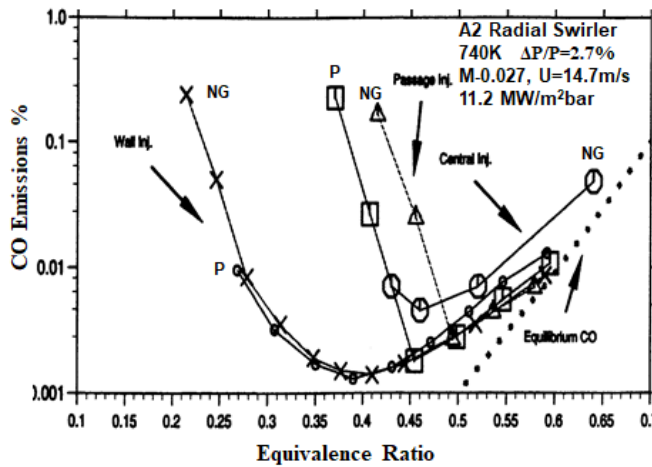
Figure 2 CO Emissions as a function of Equivalence Ratio, Ø.

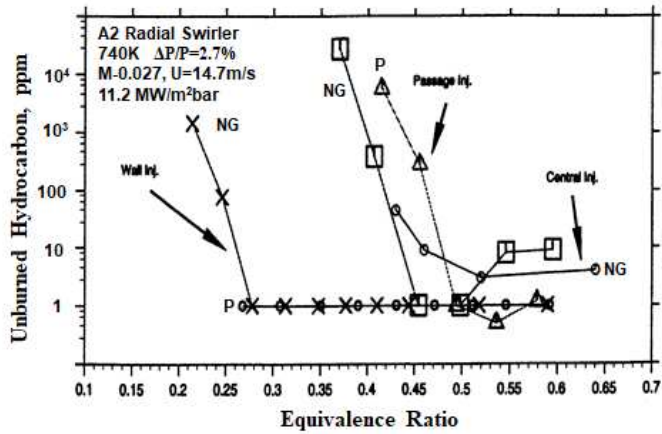Table 2 Critical Conditions for the minimum inefficiency

Fuel injection	Fuel	Air T K	$\emptyset_{crit}$ for comb. Ineff. <0.1%	Critical Flame Temp. K	NO_x 15% O_2 ppm at $\emptyset_{crit}$
Passage (1)	NG	740	0.48	1820	2
Passage (1)	NG	600	0.53	1820	9.5
Passage (1)	P	740	0.43	1820	2
Wall	NG	740	0.27	1400	14
Wall	P	740	0.27	1400	20
Central	NG	600	0.43	1760	7.5
140mm Passage (22, 23)	NG	740	0.39	1680	1.8
140mm Central (22, 23)	NG	740	0.32	1550	9

Fig. 3 THC as a function of Ø at 740K

Fig. 5 NO_x as a function of Ø
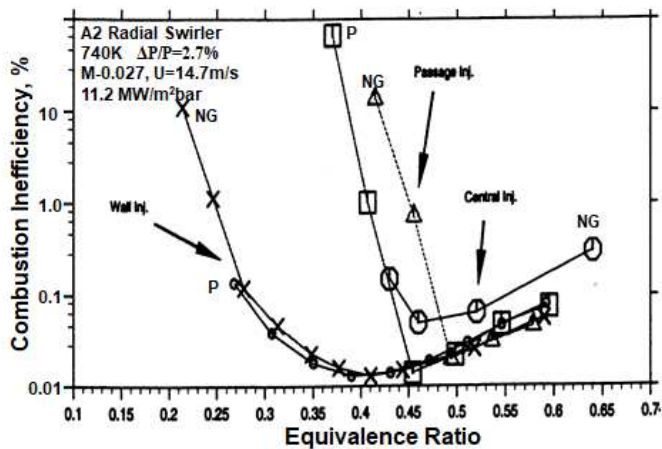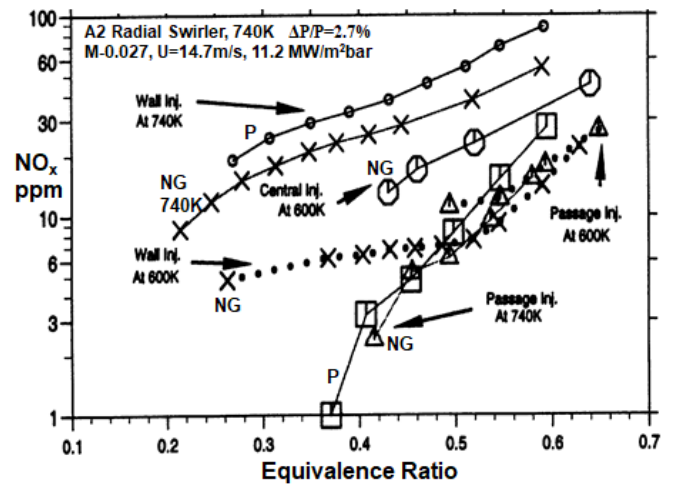
Fig. 4 Combustion Inefficiency as a function of Ø

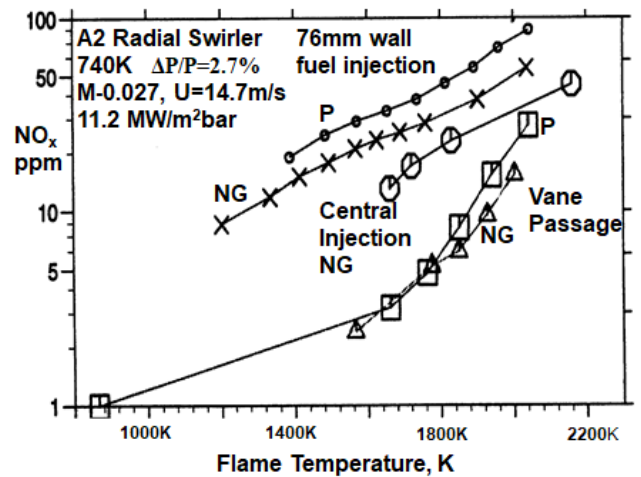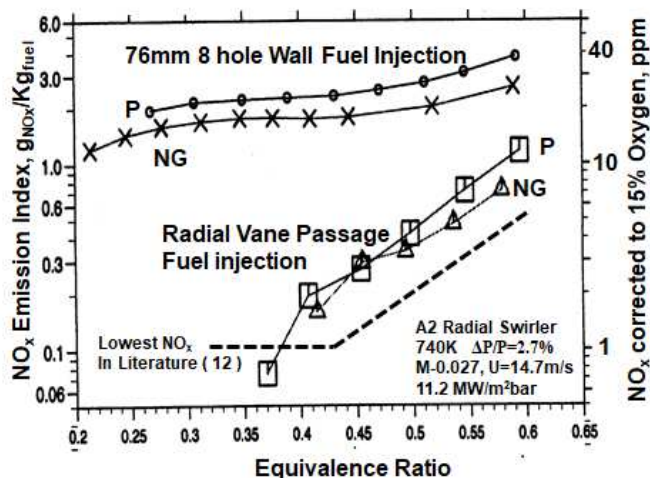

Fig. 6 NO_x as a function of the adiabatic flame temperature

5

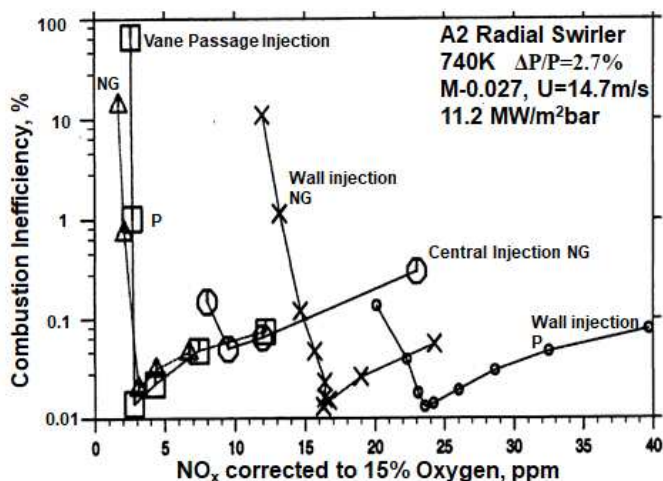Fig. 7 NO$_x$ EI g/kg and NO$_x$ corrected to 15% oxygen as a function of equivalence ratio

Fig. 8 NO$_x$ corrected to 15% oxygen as a function of the combustion inefficiency.

mixtures with the same critical Ø as for CO emissions. The combustion inefficiency is shown as a function of Ø in Fig. 4 and this has a similar shape to the CO emissions.

A minimum acceptable combustion inefficiency is 0.1% and Table 2 shows the equivalence ratio and adiabatic flame temperature at which this minimum combustion efficiency occurs for all the results. This is the minimum power turndown condition and comparison with Table 1 shows that there was a margin between the minimum combustion inefficiency Ø and the weak extinction Ø, that was sufficient for stable operation at the critical Ø to be possible. This margin was 0.14Ø and 300K for vane passage fuel injection of NG at 740K and 0.09Ø and 270K for wall fuel injection.

Table 2 also has the equivalent data for the previously published 140mm diameter combustor with 76mm diameter outlet radial swirlers (22, 23). This had the same curved radial

vane passage shape as in the present work. This comparison shows that the larger radial swirler had a much lower critical temperature of 1680K than 1820K in the present for the radial swirler with roughly half the diameter, even though the reference Mach number and pressure loss were similar. The same was the case for central injection with a critical temperature of 1760K in the present work compared with 1559K for the larger radial swirler.

The reason that the smaller size of the radial swirler could contribute to the reduced flame stability at the same pressure loss is through the length scale of turbulence, which reduces as the size of the radial passages and the combustor diameter are reduced. For the same turbulence intensity (same pressure loss) the turbulence burning velocity depends on the length scale of turbulence and this is smaller in the smaller radial swirler and so the turbulence burning velocity will be lower. The fuel and air mixing time is related to the characteristic time of the large turbulent eddies (L/u' where u' is the mean turbulent fluctuating velocity). For the same pressure loss u' is constant and so the mixing time decreases as L is reduced. This is why the smaller radial swirlers behave as more premixed than for the larger swirlers.

NO$_x$ EMISSIONS

The NO$_x$ emissions are shown as a function of Ø in Fig. 5 and as a function of adiabatic flame temperature in Fig. 6. For 740K air inlet temperature Figs. 5 and 6 show that wall fuel injection has higher NO$_x$ emissions than for vane passage fuel injection at all Ø. Thus the extension of the lean burning zone by the rich outer recirculation zone is achieved with an increase in NO$_x$. This may be acceptable at low powers if the flame is stable. Fig. 5 also compares the NO$_x$ emissions at 600K and 740K and for wall fuel injection there was a dramatic reduction in the NO$_x$ to the same level as for radial vane passage fuel injection. Wall temperature measurements showed that the distance to the peak wall temperature increased at 600K compared with 740K due to the reduced turbulent burning velocity at 600K. This indicates that the flame stabilises further downstream at 600K, which reduces the NO$_x$ with wall fuel injection due the shorter residence time in post flame gases and to a longer mixing time before the main heat release.

At 740K Fig. 6 shows that the NO$_x$ emissions for the same flame temperature are significantly higher for 76mm wall fuel injection than for vane passage fuel injection. At 1800K 5ppm for radial vane passage fuel injection increases to 30ppm for wall injection. The NO$_x$ emission index, g/kg$_{fuel}$, and NO$_x$ ppm corrected to 15% oxygen are shown as a function of equivalence ratio in Fig. 7. These results are compared in Fig. 7 with the lowest published NO$_x$ in the literature (12) for non-premixed combustion, which is based on 13 publications (12) that support this line. Fig. 7 shows that the present NO$_x$ results corrected to 15% oxygen are very close to this lowest NO$_x$ line for both NG and propane. The NO$_x$ for wall injection are higher but still below the 25ppm limit in NO$_x$ standards for NG. This means that fuel staging to the wall injection location at low

powers could be a reasonable design option. Fig. 4 shows that wall fuel injection is viable to 0.25Ø with an adequate combustion inefficiency.

The NO_x emissions corrected to 15% oxygen are shown as a function of the combustion inefficiency in Fig. 8. The minimum NO_x for a combustion inefficiency of 0.1% is shown in Table 2. For radial vane passage injection with NG 2ppm NO_x corrected to 15% oxygen was demonstrated at 1820K and this is extremely low NO_x emissions. The NO_x results at the critical condition in Table 2 show similar NO_x for the 40mm outlet diameter radial swirler compared to the 140mm radial swirler, and lower NO_x for central fuel injection. This is a result of the faster fuel and air mixing discussed above, so that the combustion was closer to premixed, which compensated for the richer Ø at the critical condition.

The increase in NO_x with wall fuel injection was to 14ppm at 15% oxygen at a critical flame temperature of 1400K, which is still quite low NO_x. The significantly higher minimum NO_x for propane was probably due to the use of the same fuel hole size for the two fuels. This would give a higher fuel injection velocity for NG than propane by a factor of 2.75 for the same total mass flow. The higher fuel velocity for NG would promote fuel and air mixing and this would lead to lower NO_x for the lean mixtures studied in the present work (12). The slightly higher peak flame temperature for propane then NG would also contribute to the higher NO_x in the diffusion combustion.

Table 2 also shows that for the same Ø the NO_x was lower in the present work than for the large 140mm diameter combustor radial swirler (22, 23). This indicates that in the smaller swirler the fuel and air were mixed better than for the larger swirler, partially due to the reduced mixing time discussed above. Part of the reason for the lower NO_x was the shape of the radial vane passages which had a narrower width and greater depth than for the larger 76mm outlet diameter radial swirlers for the 140mm combustor diameter, This would give better fuel and air mixing inside the radial vane passages for vane passage fuel injection. The inferior fuel and air mixing in the larger radial swirlers give these flames a better flame stability and hence leaner mixtures that could burn with a stable low NO_x flame with <0.1% combustion inefficiency as shown in Table 2. The greater depth of the radial swirler in Fig. 1 would also give a greater axial mixing distance before the high turbulence in the expanding swirling shear layer downstream of the dump flow expansion at the swirler exit. This was the reason for the poor flame stability with central radially outward fuel injection.

Fig. 7 shows that at 0.6Ø the NO_x would be 8ppm at 15% oxygen and this would be a typical full power condition using radial fuel injection. With pilot fuel injection at the 76mm wall 15ppm NO_x would be generated at 0.25Ø, which represents a power turndown to 40% of the peak power. This would be adequate to meet the required power turndown range for MGTs and so a pilot/main operation with the main using radial vane passage fuel injection at high powers with the 76mm wall pilot fuel injection acting in a dual fuel mode at low powers. Andrews and Mkpadi (34) have shown that the combination of pilot and main fueling enable the main flame to burn at leaner mixtures with pilot fueling present and so stable combustion from 0.25 – 0.6Ø would be expected in the present work with pilot/main combustion with low (<15ppm) NO_x across the power range 40 – 100% power range.

CONCLUSIONS

A low NO_x radial swirler for combustor sizes of the order of 140mm diameter (12-15), that has several industrial applications (11, 27, 28, 30), has been successfully scaled down to a 76mm diameter MGT application with a single combustor. At 0.6Ø for full power the combustion intensity was 11.2 MW/(bar m^2) for a primary zone Mach number of 0.027, corresponding to 54% of the combustion air passing through the swirler. This is a smaller combustor and much higher combustion intensity than any current MGT. A single combustor for MGT applications with a pressure ratio of 5 bara [25, 26] and simple cycle thermal efficiency of 0.3 [25, 26], would give a MGT with 77kWe power output.

Andrews and Kim (1) showed that the small radial swirler, with radial vane passage single hole fuel injection at the passage inlet, had low NO_x at <10ppm corrected to 15% oxygen over a wide range of Ø from 0.4 to 0.6 for NG. The NO_x emissions were comparable with the lowest in the literature for the same flame temperature. The better mixing that gave this lower NO_x reduced the flame stability to close to that of premixed systems (1) and this reduced the power turndown capability. To improve the power turndown of the small radial swirler with vane passage fuel injection, two pilot fuel injection locations were investigated: central 8 hole radially outward fuel injection and a 76mm wall pilot fuel injector into the outer recirculation zone at the swirler dump expansion.

An eight hole radially outward central pilot fuel injector was shown to deteriorate the weak extinction compared with radial vane passage fuel injection and was rejected as a pilot fuel location. This was unexpected, as in the larger 140mm combustor format central fuel injection was a successful pilot fuel location. It was concluded that the greater depth of the 40mm outlet diameter swirler, relative to the 76mm outlet diameter swirler, gave a greater distance between the central fuel injector and the dump expansion swirling shear layer and this gave enhanced fuel and air mixing.

The fuel injection at the 76mm combustor wall just downstream of the 40mm swirler outlet dump flow expansion was shown to be a successful pilot fuel injection location. This enabled the flame stability to be improved and operation was demonstrated with <1% combustion inefficiency at 0.25Ø compared with 0.48Ø for radial vane passage fuel injection. The NO_x increased, but was still significantly below the 25ppm regulation limit. This would enable power turndown on the MGT to be achieved with low NO_x and low CO and HC emissions, sufficient for MGT power operation range.

REFERENCES

[1] Andrews, G.E. and Kim, M., Small radial swirler low NO$_x$ combustors for micro gas turbine applications. Proceedings of the ASME Turbo Expo:Turbomachinery Technical Conference & Exposition GT2017 June 26 - 30, 2017, Charlotte, North Carolina, USA. ASME Technical Paper GT2017-63494

[2] European Commission, 2014. "Strategic Energy Technology (SET) Plan Towards an Integrated Roadmap: Research & Innovation Challenges and Needs of the EU Energy System". JRC 93056.

[3] Cameretti, M.C., Ferrara, F., Gimelli, A. and Tuccillo, R., 2015. "Employing Micro-Turbine Components in iIntegrated Solar-MGT-ORC Plants. Proc. ASME Turbo Expo 2015, Montreal, Canada. ASME Paper GT2015-42572.

[4] Shixi, M., Zhou, D/, Zhang, H. and Lu, Z., 2016. "Micro Gas Turbine/Renewable Hybrid Power System for Distributed Generation: Effects of Ambient Conditions on Control Strategy. Proc. ASME Turbo Expo 2016, ASME Paper GT2016-57564.

[5] Chiaramonti, D., Riccio, G.and Martelli, F., 2004. "Preliminary Design and Economic Analysis of a Biomass FED Micro Gas Turbine Plant for Decentralised Energy Generation in Tuscany". Proc. ASME Turbo Expo, 2004. ASME Paper GT2004-53546.

[6] Zampilli, M., Bidini, G., Laranci, P. and Fantozzi, F, 2016. "Externally Fired Gas Turbine: Layout Optimization for Micro CHP Generation with Residual Biomass Firing". Proc. ASME Turbo Expo, Seoul, S. Korea. ASME Paper GT2016-57969.

[7] Buhre, B.J.P. and Andries, J., 2000."Biomass-based, Small-scale, Distributed Generation of Electricity and Heat Using Integrated Gas Turbine-Fuel Cell Systems". Prof. ASME Turbo Expo 2000. ASME Paper 2000-GT-0083.

[8] Tan, F.X., Rajoo, S., Chiong, M.S., Chong, C.T., Romagnoli, A. and Ochiai, M., 2015. "Design of Micro Gas Turbine System using Commercial Turbocharger". Proc. Int. Gas Turbine Congress, 2015, Tokyo, p.102-108.

[9] Vick, M., Young, T., Kelly, M., Tuttle, S. and Hinnant, K., 2016. "A Simple Recuperated Ceramic Microturbine: Design Concept, Cycle Analysis and Recuperator Component Prototype Tests". Proc. ASME Turbo Expo 2016, Soeul, S. Korea. ASME Paper GT2016-57780.ve

[10] Phi, V.M., Mauzey, J.L., McDonell, V.G. and Samuelsen, G.S., 2004. "Fuel Injection and Emissions Characteristics of a Commercial Microturbine Generator". Proc.ASME Turbo Expo 2004, Vienna, Austria. ASME Paper GT2004-54039.

[11] Armstrong, J., Bolin, C., Ebrahim, M. and Carney, M., 2016. "Development and Testing of a 333kW Industrial Gas Turbine". Proc. ASME Turbo Expo 2016, Seoul, S. Korea. ASME Paper GT2016-57828.

[12] G.E. Andrews, 2013. "Ultra low nitrogen oxides (NO$_x$) emissions combustion in gas turbine systems". Chapter 16 In: Modern Gas Turbine Systems, Ed. Peter Jansohn, Woodhead Publishing. pp.715-790. ISBN 978-1-84569-728-0. DOI:10.1533/9780857096067.3.715

[13] Alkabie, H.S., Andrews, G.E. and Ahmad, N.T., 1988. "Lean low NO$_x$ primary zones using radial swirlers". Proc. ASME Turbo Expo 1988, Amsterdam. ASME Paper 88-GT-245.

[14] Alkabie, H.S. and Andrews, G.E., 1989. "Ultra-low NO$_x$ emissions for gas and liquid fuel using radial swirlers" Proc. ASME Turbo Expo 1989, Toronto. ASME Paper 89-GT-322.

[15] Alkabie, H.S. and Andrews, G.E., 1990. "Radial swirlers with peripheral fuel injection for ultra-low NO$_x$ emissions". ASME Turbo Expo, 1990, Brussels. ASME Paper 90-GT-102.

[16] Kim, S., Andrews, G.E. and Alkabie, H.S., 1993. "An ultra-low NO$_x$ pilot combustor for staged low NO$_x$ designs". Proc. Eleventh International Symposium on Air Breathing Engines (XI ISABE).

[17] Seki, K., Nakano, S. and Takeda, Y., 2015. "Dynamic Simulations for a Microturbine". Proc. Int. Gas Turbine Congress, 2015, Tokyo, p.478-484.

[18] Monz, T.O., Stohr, M., O'Loughlin, W., Zanger, J., Hohloch, M. and Aigner, M., 2015. "Experimental Characterisation of a Swirl-Stabilized MGT Combustor". Proc. ASME Turbo Expo 2015, Montreal, Canada. ASME Paper GT2015-42387.

[19] Parente, J., Mori, G., Anisimonv, V.V. and Croce, G., 2004. "Micro Gas Turbine Combustion Chamber Design and CFD Analysis". Proc. ASME Turbo Expo, 2004, Vienna, Austria. ASME Paper GT2004-54247.

[20] Cameretti, M.C. and Tuccillo, R., 2004. "Comparing Different Solutions for the Micro-Gas Turbine Combustor". Proc. ASME Turbo Expo 2004, Vienna, Austria. ASME Paper GT2004-53286.

[21] Riccio, G., Piazzini, S., Adami, P., Martelli, F., Tanzini, G., Carrai, L. and Spadi, A., 2004. "Development and Experimental Testing of a Pilot Burner for DLN Combustors". Proc. ASME Turbo Expo 2004. ASME Paper GT2004-53513.

[22] Escott, N.H., Andrews, G.E., Alkabie, H.S., Al-Shaikhly, A.F. and George, B., 1993. Large airflow capacity radial swirlers for ultra low NO_x at high inlet temperatures. Proceedings of ASME Seventh International Congress and Exposition on Gas Turbines in Cogeneration, Utility, Industrial and Independent Power Generation, Vol. 8, ASME COGEN TURBO '93, pp. 241-243.

[23] Andrews, G.E., N. Escott, and M.C. Mkpadi, 2008. "Radial swirler designs for ultra low NOx gas turbine combustion". ASME Turbo Expo 2008, Germany. ASME Paper GT2008-50406.

[24] Andrews, G.E. and Ahmad, N.T., 2011. "Axial Swirler Design Influences on NO_x Emissions for Premixed Combustion in Gas Turbine Combustors with all the Combustor Air Flow Passing Through the Swirler". Proc. ASME Turbo Expo 2011, Vancouver, Canada. ASME Paper GT2011-45418.

[25] Jaatinen-Varri, A., Nerg, J., Uusitalo, A., Ghalamchi, B., Uzhegov, N., Smirnov, A., Sikanen, E., Gronman, A., Backman, J., Malkamaki, M., 2016. "Design of a 400kW Gas Turbine Prototype". Proc. ASME Turbo Expo, 2016. Seoul, S. Korea. ASME Paper GT2016-56444.

[26] Henke, M., Klempp, N., Hohloch, M., Monz, T. and Aigner, M., 2015. "Validation of a T100 Micro Gas Turbine Steady-State Simulation Tool". Proc. ASME Turbo Expo 2015, Montreal Canada. ASME Paper GT2015-42090.

[27] Fischer, S., Kluss, D. and Joos, F., 2015. "On the Influence of Fuel Mixing and Flue Gas Recirculation on the Emissions of a Fuel Flexible Gas Turbine Combustor". Proc. ASME Turbo Expo 2015, Montreal, Canada. ASME Paper GT2015-42373.

[28] Boyns, M.B. and Patel, R., 1997. "The Application of DLN Technology to the Tornado and Tempest Industrial Gas Turbines". ASME Turbo Expo 1997, Orlando, USA. ASME Paper 970GT-059.

[29] Alkabie, H.S. and Andrews, G.E. The influence of fuel placement on NO_x emissions from flames stabilized by radial swirlers, Proceedings of the Tenth International Symposium on Air Breathing Engines (10th ISABE), AIAAm vol.1, pp.411-420, ISBN 1-56347-006-3 (1991).

[30] Willis, J.D., Toon, I.J., Schweiger, T. and Owen, D.A., 1993. "Industrial RB211 Dry Low Emission Combustor". ASME Paper 93-GT-391.

[31] Scarinci, T., Freeman, C. and Day, I., 2004. "Passive Control of Combustion Instabilities in a Low Emission Aeroderivative Gas Turbine". ASME Paper GT2004-53767.

[32] Bauerheim, M., Jaravel, T., Esclapez, L., Riber, E., Gicquel, L.Y.M., Cuenot, B., Cazalens, M., Bourgois, S. and Rullaud, M, 2015. "Multiphase Flow LES Study of the Fuel Split Effects on Combustion Instabilities in an Ultra Low NOx Annular Combustor". Proc. ASME Turbo Expo, Montreal, Canada. ASME Paper GT2015-44139.

[33] Andrews, G.E., Ahmed, N.T., Phylaktou, H.N. and King, P., 2009. "Weak Extinction in Low NOx Gas Turbine Combustors". Proc. ASME Turbo Expo 2009, Orlando, Florida. ASME Paper GT2009-59830.

[34] Andrews, G.E. and Mkpadi, M.C., 2001. "High turndown ratio, low NO_x gas turbine combustion", ASME Paper 2001-GT-59. Proceedings of the ASME International Gas Turbine & Aeroengine Congress & Exhibition, New Orleans.

Correspondence:
Professor Gordon E. Andrews
profgeandrews@hotmail.com
<G.E.Andrews@leeds.ac.uk>